TILT *c* AXIS CRYSTALLITE GROWTH OF ALUMINIUM NITRIDE FILMS BY REACTIVE RF-MAGNETRON SPUTTERING

G. E. STAN[a,*], I. PASUK[a], L. M. TRINCA[a], A. C. GALCA[a],
M. ENCULESCU[a], F. MICULESCU[b]
[a]*National Institute of Materials Physics, P.O. Box MG-7, Bucharest-Magurele, 077125, Romania*
[b]*Politehnica University of Bucharest, Faculty of Materials Science and Engineering, Bucharest, Romania, Bucharest 060042, Romania*

The article reports on the tilted growth of textured aluminium nitride thin films obtained by radio-frequency magnetron sputtering onto 50 mm diameter Si (111) wafers, in reactive atmosphere, in a planar sputtering system without tilting the substrate and with no additional sputtering geometry alterations. The films were investigated using, X-ray diffraction, spectroscopic ellipsometry and scanning electronic microscopy, done by local measurements on the wafer surface, at different distances from the centre. A progressive increase of the tilt angle when moving away from the sample centre has been found. The maximum tilt angle of the columnar AlN crystallites, obtained near the edges of the wafer, is about 7°. The results showed also that tilting is associated with smaller thickness and larger dispersion of the *c* axis orientation. Synthesizing inclined *c* axis AlN films should allow the fabrication of surface acoustic wave devices based on shear waves for liquid sensor applications.

1. Introduction

Aluminium nitride (AlN) has been extensively studied in the past decade due to its unique properties such as: wide energy band gap (6.2 eV), high surface acoustic velocity (up to 6000 m/s), high breakdown voltage, high electrical resistivity (~10^{15} ohm·cm), high hardness (11–15 GPa), high piezoelectric coupling factor, thermal and chemical stability, high thermal conductivity, and high corrosion resistance [1,2].

Most recently due to a growing interest for the wireless communication systems working at high frequency and high accuracy biochemical sensing devices, the micro and nano-sized piezoelectric AlN thin films-based devices have drawn continuous and significant attention [3–5]. Certainly the most popular, reliable and low-cost deposition method for qualitative AlN thin films is constituted by reactive magnetron sputtering [6–8]. The progress in optimizing the quality of AlN thin films in terms of structure (crystallinity and degree of texturing), surface morphology and piezoelectric coefficient led to the fabrication of devices with superior functionality [9–11].

The high c-axis texturing of the AlN films is of great importance, assuring the excitation of pure longitudinal mode along their thickness direction, and determining optimal piezoelectricity, electro-mechanical coupling coefficient and acoustic velocity response. However, in case of biochemical sensors operating in liquid media the longitudinal waves produce a compression-type motion elapsing acoustic energy into the liquid media, and resulting in a reduced resolution. Therefore, a shear-mode resonance instead of longitudinal-mode resonance is required

---

* Corresponding author: george_stan@infim.ro

for biochemical sensors, as the fading of shear-mode acoustic wave is not so severe in liquid media.

AlN films having tilted texture posses the capability to excite both longitudinal and shear mode resonance. The full compatibility with the current microelectronics requires a low temperature deposition process. However, the synthesis of highly *c*-axis textured AlN films at low temperature is still challenging. The preparation of highly *c*-axis textured AlN thin films often requires a high substrate temperature. Reactive radio-frequency magnetron sputtering (RF-MS) presents the advantage of low deposition temperatures (usually bellow 150°C), and could allow the synthesis AlN films with preferred crystal orientations and reduced roughness at low pressure [3,4]. The generation of shear waves is believed to be induced for the *c*-axis inclinations ranging between 5° and 30° [12,13].

This study is the first from a series attempting to propose a low temperature magnetron sputtering deposition regime for obtaining tilted grown AlN thin films and study its technological suitability. A low temperature process would allow low mobility of ad-atoms on the substrate surface favouring tilted grain growth, and in the same time is compatible with the current microelectronics processing. The studies could be of significance in view of fabricating a new generation of surface acoustic wave devices operating as liquid sensors.

2. Experimental

2.1 *Deposition procedure*

The AlN films were synthesized using a UVN-75R1 sputtering deposition system equipped with planar water-cooled magnetron cathodes (110 mm diameter). An aluminium disc (Angstrom Sciences, Inc., 99.999 % purity, 3 mm thick) was used as a cathode target. 50 mm diameter silicon (111) wafers were chosen as deposition substrates. Before the introduction into the deposition chamber, the substrates were successively cleaned ultrasonically in acetone and ethanol for 10 min in a NAHITA 610/6 ultrasonic bath. The target-to-substrate distance was set at 35 mm. In a first step, the sputtering chamber was evacuated down to a base pressure of 10^{-4} Pa. Further on, high purity argon (99.99%) was introduced through a needle valve and the gas flow was maintained at a value of 45 sccm. The target was sputter-cleaned at a working pressure of 0.3 Pa for 15 minutes to remove surface contaminants. During cleaning, the substrates were masked with a stainless steel shield in order to avoid undesired depositions onto the substrates' surface. Prior to deposition, the substrates were etched for 10 min, at a 0.4 kV DC bias voltage in argon plasma produced by a wolfram plasmatron, in order to remove the thin native oxide layers and other impurities which might persist after the ultrasonic cleaning. This substrates' treatment is known to increase films' adhesion and reduce the possibility of delamination [14]. The disc shaped wafers were positioned in such a way that the deposition centre approximates the specimen centre.

We used a radio-frequency (1.78 MHz) generator and maintained a constant and low RF power (100 W) in order to avoid overheating of the target surface. A plasma ring of about 55 mm diameter was generated by the planar magnetron cathode. The sputtering was carried out for 1 hour in 0.2 Pa Ar-N₂ gas mixture with a nitrogen concentration of 25%. The substrates were not heated during deposition and their temperature was only dependent on plasma self-heating, reaching for our sputtering conditions ~ 50°C.

2.2 *Characterization of AlN sputtered films*

After deposition the specimens were studied thoroughly from structural and optical point of view. In order to emphasize the AlN film growth dependence on substrate area, local measurements were performed in steps of 2.5 mm starting from the deposition centre. Due to the radial symmetry of the magnetron sputtering geometry, the analyzed areas were selected only along the wafer diameter. The crystallographic structure of each film was analyzed by X-ray diffraction (XRD) on a *Bruker D8 Advance* diffractometer in parallel beam setting, equipped with

Cu target X-ray tube with linear focus. The goniometer setting include a two bounce Ge (022) monochromator, assuring a monochromatized $CuK_{\alpha 1}$ radiation ($\lambda = 1.5406$ Å). A home-made circular slit has been put in the incident beam, in order to restrain the axial expansion of the spot on the sample surface. The obtained spot is almost circular with a diameter of about 2 mm at the incidence angle corresponding to the 002 peak of AlN. The optical measurements were done with a *Woollam* Variable Angle Spectroscopic Ellipsometer (*VASE*) system, equipped with a high pressure Xe discharge lamp incorporated in an *HS-190* monochromator. Measurements are performed in the IR-Vis-UV region of the spectrum at energies between 1 and 6.2 eV, step of 0.01 eV, at 45°, 60° and 75° angles of incidence. The growth morphology of the films was examined using scanning electron microscopy (*Carl Zeiss EVO 50 XVP*; 30 kV acceleration voltage and 10 µA beam current) under secondary electron mode, in cross-view mode on the fractured samples.

3. Results and discussion

3.1 XRD results

The XRD diagrams, obtained in symmetric (Theta-Theta) scan, present only two peaks given by the film structure, corresponding to the 002 and 004 reflections of hexagonal AlN (Fig. 1). The absence of any other AlN peaks in the whole accessible scanning range points to the highly *c* axis oriented growth of the films.
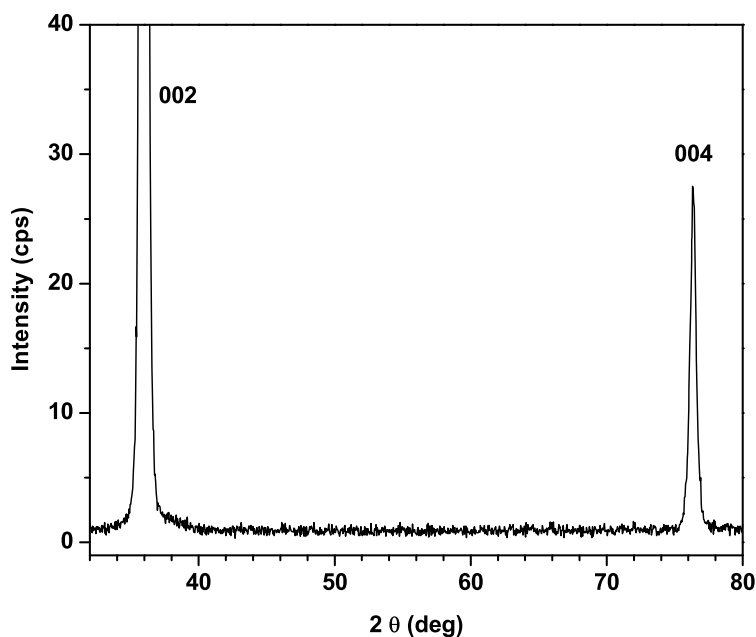

Fig. 1. XRD Theta-Theta scan of the film deposited on Si (111) wafer

The Bragg angles did not vary with the location of the area investigated: $2\theta_{B\ 002} = 36.02°$, $2\theta_{B\ 004} = 76.37°$, showing that the periodicity along the *c* axis is the same in each point of the surface: $c = 4.983$ Å.

Rocking curves (ω scans) were registered at each measurement point, with the scattering angle fixed to $2\theta_{B\ 002}$, in order to determine the tilt angle of the (001) AlN planes with respect to the sample surface, τ (Fig. 2 and Fig. 3). The measurement points are labelled with L and R at the left hand side and at the right hand side of the centre, respectively. Left hand side means the sample side closer to the X-ray tub, and right hand side - the sample side closer to the detector. The ω_0 positions of the rocking curves decrease monotonously from 24.62° at the leftmost point of the surface to 11.73° at the rightmost point, passing through $\omega_0 = \theta_B = 18.01°$ in the deposition centre (Fig. 2).
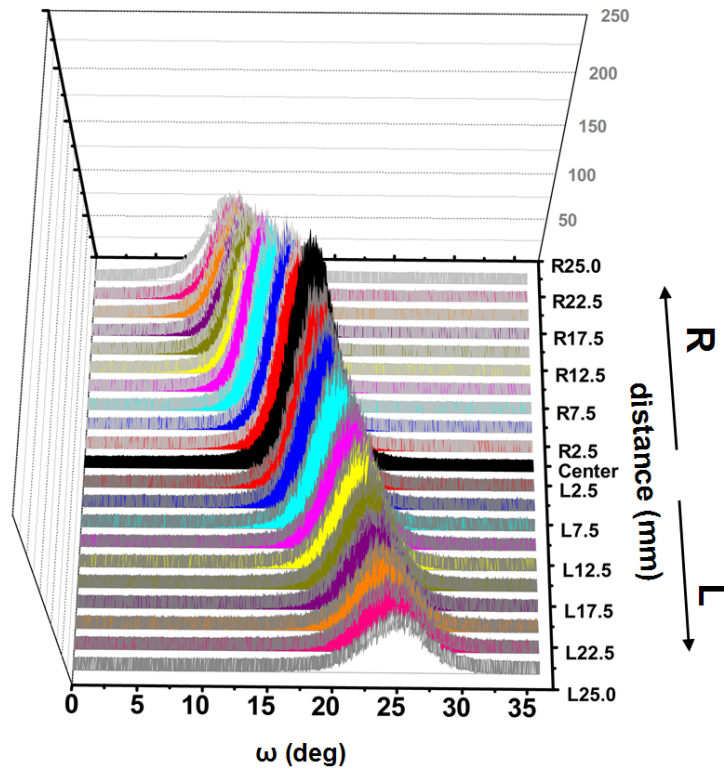
Fig. 2. Rocking curves corresponding to the 002 AlN peak ($2\theta_{B\ 002}$ = 36.02°). Lx and Rx indicate the position where the rocking curve was collected, at spacing x from the deposition centre, at the left (L) and right (R) hand side of the sample, respectively

The value of the tilt angle is connected to ω_0 by the equation:

$$\tau = \omega_0 - \theta_B, \tag{1}$$

where θ_B is the Bragg angle characteristic to the crystal plane family (Fig. 3).

The experiments showed that at the left hand side the incidence angle of the beam on the surface must be higher than θ_B to satisfy the reflection condition for the 002 AlN peak, while on the right hand side, the incidence most be smaller than θ_B (Fig. 3). Thus at the left hand side the tilt angle of the crystallites have positive values, $\tau > 0$, while at the right hand side $\tau < 0$, giving rise to a flower bud like structure of the overall specimen.
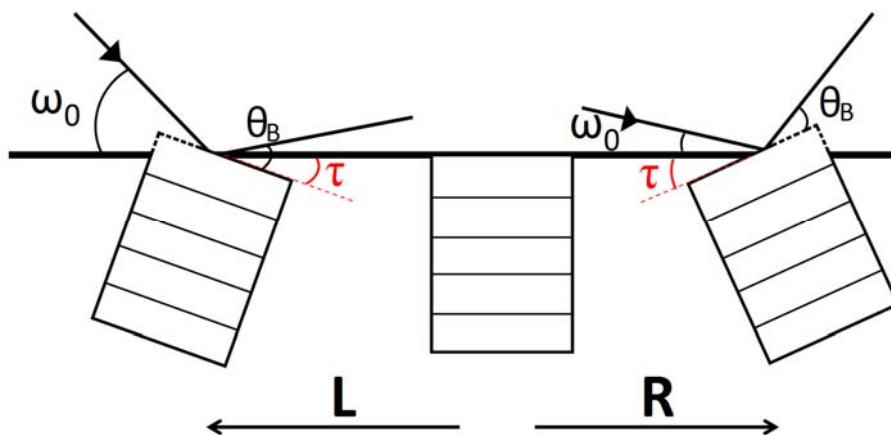

Fig. 3. Schematic representation of the rocking curve measurement geometry and of the flower-bud symmetry of the AlN film structure

The tilt angles calculated with equation (1) are represented versus the distance from centre in Fig. 4, where the negative, right hand side, values were represented in module, to better suggest the symmetry of the specimen structure. The dependence is practically linear. One can believe that the radial symmetry of the deposited specimen structure is related to typical geometry of the sputtering deposition.
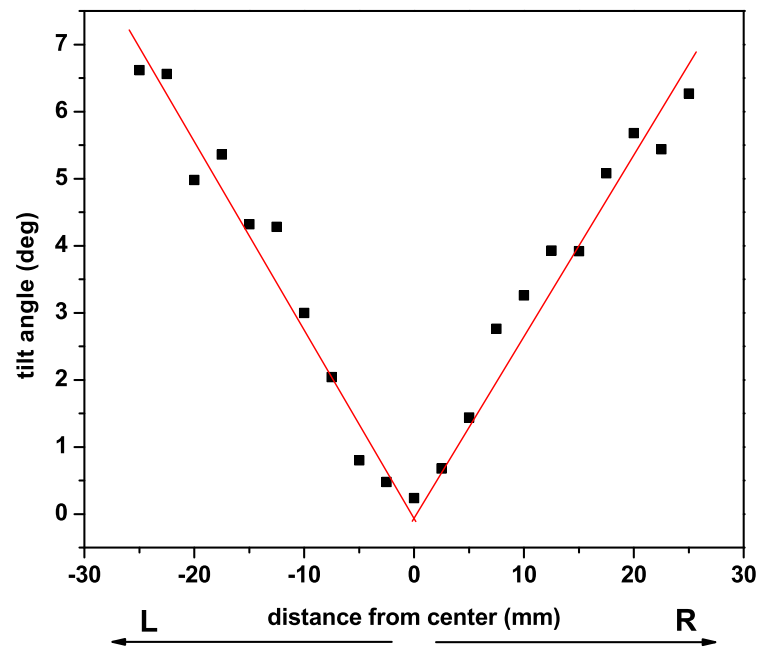

Fig. 4. Tilt angle, τ, vs. distance from the centre of the interference rings

Fig. 2 shows that the shape and intensity of the rocking curves also vary with the measurement point. The full width at half maximum (FWHM) increases towards the extremity of the sample (Fig. 5a), and the area below the curve decreases (Fig. 5b).
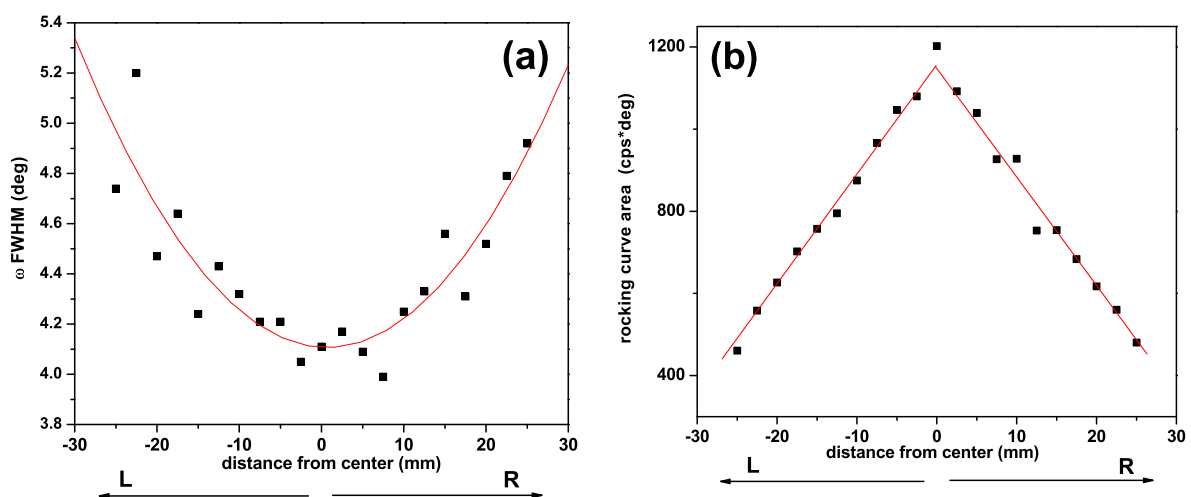

Fig. 5a. Rocking curve breath vs. measurement point

Fig. 5b. The integral intensities of the rocking curves vs. measurement point

The FWHM of the rocking curves is due to the spread of the orientations of the crystallites, around the most probable direction. The area under the rocking curves, namely their integral intensities, is determined by the total number of the crystallites contributing to the scattering at the given area of measurement on the sample surface. Earlier study on RF-MS AlN films [15] demonstrated that the smaller the film thickness, the broader is the *c* axis orientation. Thus, both curves in Fig. 5 indicate that the film thickness decreases towards the edges of the sample. This finding is well correlated with the results of spectroscopic ellipsometry to be presented hereafter. An additional hypothesis is that the degree of AlN *c* axis orientation is diminished to the wafer edges also due to the cosine law distribution of sputtered particles [16] that influences the diffusion ability of the ad-atoms which in turn governs the film's crystallization.

3.2 Spectroscopic Ellipsometry (SE) measurements

SE is used to determine the thickness and optical properties of the deposited thin film. The experimental data is expressed by the ellipsometry quantity ρ given by:

$$\rho = \frac{r_p}{r_s} = \frac{\vec{E}_p^r}{\vec{E}_s^r} \cdot \frac{\vec{E}_s^i}{\vec{E}_p^i} = \tan \Psi \exp(i\Delta), \tag{2}$$

where r_p and r_s are the Fresnel reflection coefficients for parallel and perpendicular polarization, respectively; in the equation (2) are represented also the electric fields of the incident and reflected light. Furthermore the elliptically polarized light reflecting from the surface is characterized by the two angles Ψ and Δ. Since the two mentioned angles are only properties of the reflected light, for getting physical parameters of the sample an accurate optical model is needed, which enables the fitting of the results.

In our case, the crystalline anisotropy of AlN induces also a slight optical anisotropy. The difference between the refractive indices along *c* axis and perpendicular on it, respectively, $n_c - n_a$, is in the Vis –NiR spectral range approximately 0.05.

To model the AlN thin film, we used a uniaxial anisotropic model with an out-of-plane refractive index n_e (extraordinary direction) different from the refractive index n_o parallel to the sample surface (the ordinary direction). Both refractive indices are Cauchy dispersions. The completely optical model consists of Si substrate, the anisotropic AlN thin film and the top surface roughness.

For an accurate characterization the experimental data were constrained between 0.7 and 3 eV and only taken at a 45° angle of incidence due to the following reasons:

i)   To avoid the Urbach tail observed in impure crystals, polycrystalline films and disordered materials. This absorption tail occurs below the band gap and can influence the quality of fitting the data by using a Cauchy dispersion (used only for fully transparent materials);

ii)   To enhance the sensitivity of the experimental data on the anisotropy. The r_s Fresnel coefficient is given only by the in-plane refractive index n_o, whereas r_p depends both on n_o and n_e. Although the sensitivity of the experimental data is not diverted by the used angle of incidence, the fitting routine should be more precise at lower angles of incidence since the contribution of n_e on r_p is larger.

iii)   To analyze the reflected beam from the same and small measured area. The incident beam of used ellipsometer has the section diameter of approximately 2 mm. The analyzed surface increases as the incidence angle increase, and therefore the

experimental data collected at different angles of incidence might differ if the thin film properties are not the same all over the sample surface.
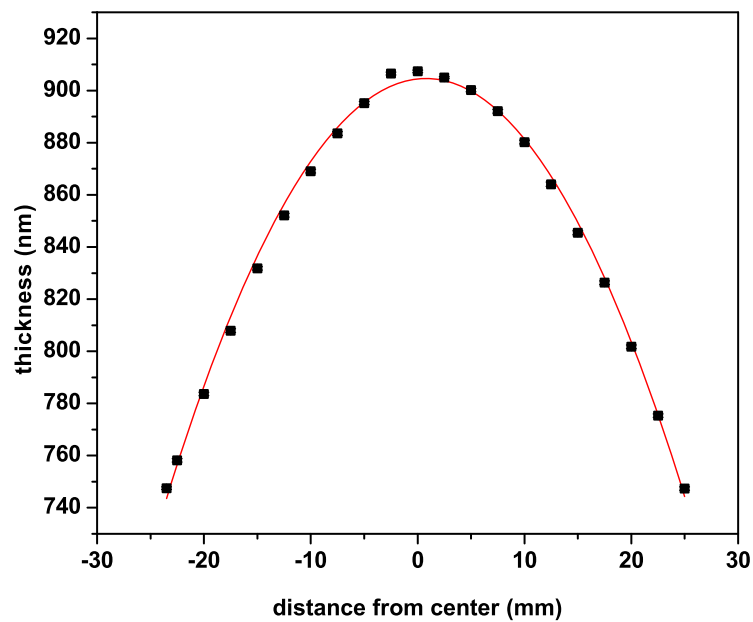

Fig. 6. The film thickness value vs. measurement point

In Fig. 6 it is presented the thickness line profile of the AlN sample. The rate of thickness decrease is approximately 8 nm/mm. The monotonous decrease of film thickness with the distance from the centre is determined by the cosine distribution law of the sputtered particles. For magnetron sputtering the cosine distribution implies that a higher number of particles is sputtered at lower exit angles (angle between the sputtered particle and the horizontal surface), fewer and fewer particles being sputtered at larger exit angles.
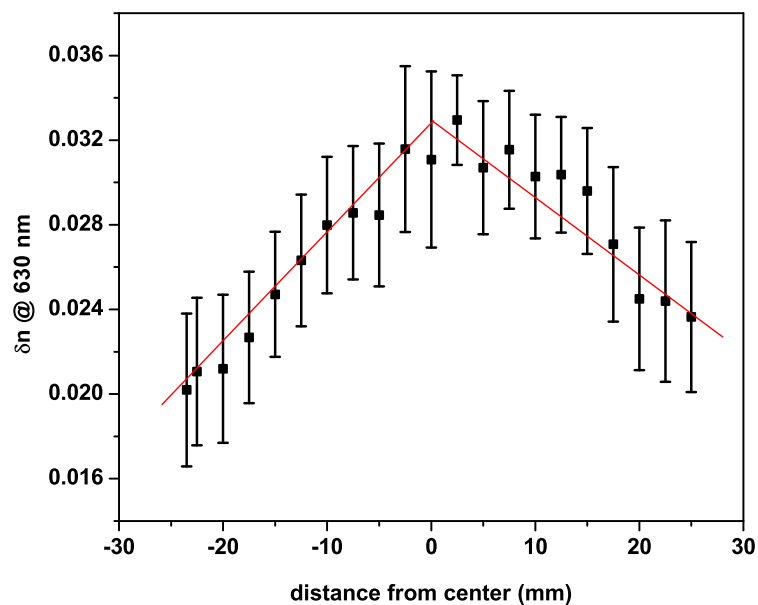

Fig. 7. The birefringence at 630 nm wavelength profile and the associated fitting errors of the analyzed sample

In Fig. 7 is shown the birefringence, $\partial n = n_e - n_o$, profile along an arbitrary direction. At the same wavelength value of 630 nm, n_e has values between 2.11 and 2.095 whereas n_o is ranged between 2.069 and 2.078. It can be observed that in the central part of the sample the birefringence is higher than the ones on the edges. Without any information from complementary techniques, this change in birefringence can be assigned to different distribution of c axis alignment along the normal to the surface, or to different orientation of the c axis with respect to the normal to the surface. In an ideal case, a single crystal thin AlN film deposited on a substrate, the birefringence values would be the same and with maximum values. In our case in the central part of the sample where the crystallites alignment is the best, there is still a distribution of c axis orientation with respect to the normal to the surface proven by XRD rocking curves (Figs. 2&4). Therefore n_e will be smaller than n_c, and n_o greater than n_a, resulting with a smaller birefringence than an ideal case. If the c axis crystallites are tilted, then the birefringence will become even smaller, as in the case of our sample.

3.3 SEM analysis

The cross-sectional SEM micrographs were collected in few film regions to check the AlN films' growth morphology and inclination (Fig. 8). A columnar-type microstructure was noticed, the film having a thickness of ~ 0.9 μm (data not presented), in good agreement with the SE results.
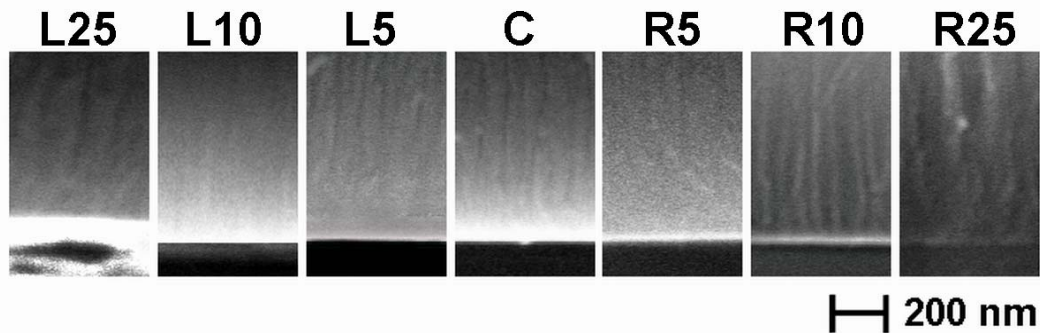

Fig. 8. Cross-sectional SEM views of the AlN reactive sputtered film onto Si (111) wafer

One can notice the "flower-bud" type morphology for the AlN film, the columns' inclination followed the inclination of *c axis* crystallites already demonstrated by the aforementioned XRD results. In the centre of the wafer the AlN film presents a perfectly vertical alignment of the columns. The columns start to tilt from a distance to the centre of about 5 mm, their speed of inclination did not vary remarkably up the edges. A slightly higher inclination was evidenced for the columns with respect to the c axis crystallites tilt (Figs. 4,7&8). The columns revealed by SEM had a maximum tilt of below 10° at the sample edges in good agreement with XRD results.

The c axis crystallites inclination is due to the oblique incidence of the impinging flux, attributed to the cosine distribution of the sputtered particles [16,17]. On the other hand, the ad-atoms' mobility is playing a crucial role in generating the tilt grain growth in AlN thin films as well as in determining the out-of-plane texture. For instance an increased ad-atom mobility determined by a high substrate temperature would allow the development of the AlN microstructure almost independent of deposition direction. In our case, by tailoring the deposition conditions (low total pressure – 0.2 Pa and low substrate temperature ~ 50°C) low mobility ad-atoms were created, their positions being easily blocked during deposition, allowing the texture of deposited film to pivot in the sputtered flux direction [18–20].

Therefore, inclination of the *c axis* crystallites is facilitated both by the oblique atoms incidence at different distances from the centre and by the low substrate temperature, which do not assure enough energy for surface mobility of the ad-atoms and their re-arrangement in the minimum energy sites. A low temperature deposition can be also very important in view of device processing. Regarding the progressive tilting of AlN columns with the distance from the radial symmetry centre of the film one cannot neglect also the role of shadowing effect owned to the oblique-incidence sputtering [21,22].

4. Conclusions

The deposition of AlN films with c-axis tilted crystallites was successfully carried out by using an RF magnetron sputtering planar system under low pressure (0.2 Pa), nitrogen dilution (25%) and temperature (50°C) conditions in view of fabricating shear-based excitation surface acoustic wave devices working as liquid sensors. The crystalline orientation and the inclination of the *c* axis crystallites of the obtained AlN films were checked and thoroughly investigated using X-ray diffraction rocking curves, spectroscopic ellipsometry and scanning electronic microscopy. These structural and optical analyses revealed that the (001) textured AlN film is not uniformly tilted all-over the surface of a Si(111) wafer of 50 mm diameter. No *c* axis crystallites or column inclination was noticed in the central region of the specimen, but the crystallites are inclined all-over in the rest. The tilt angle increases linearly with the distance from the deposition centre, such that the overall film structure on the wafer got a flower-bud like symmetry. The maximum tilt, measured by XRD in the marginal areas of the wafer was about 7°. A thickness variation of about ±18% was recorded for the AlN film at the edges of the wafer (at a distance from centre of 25 mm).

The results suggest that one can obtain AlN films with a designed oblique texture by positioning the substrate in a given off-centre position during deposition, with no need for tilting of the substrate or other sputtering geometry alterations. Depending on the RF-MS growth conditions, the AlN film can respond to the incident atoms by tilting the *c* axis toward the deposition direction. A low deposition pressure provides sputtering atoms with sufficient kinetic energy to arrange in (*001*) plane resulting in a well-textured film, while a low temperature hinders the transverse diffusion of the ad-atoms on the surface, favouring the tilted growth of the film.

References

[1] Ioffe data archive: http://www.ioffe.rssi.ru/SVA/NSM/Semicond/AlN/index.html
[2] L. I. Berger, Semiconductor materials, CRC Press (1997).
[3] V. Cimalla, J. Pezoldt, O. Ambacher, J. Phys. D: Appl. Phys. **40,** 6386 (2007).
[4] P. Muralt, J. Am. Ceram. Soc. **91**, 1385 (2008).
[5] S. Tadigadapa, K. Mateti, Meas. Sci. Technol. **20**, 092001 (2009).
[6] G. F. Iriarte, J. Vac. Sci. Technol. A **28**, 193 (2010).
[7] M. V. Pelegrini, I. Pereyra, Phys. Status Solidi B 7, 840 (2010).
[8] G. F. Iriarte, D. F. Reyes, D. González, J. G. Rodriguez, R. García, F. Calle, Appl. Surf. Sci. **257**, 9306 (2011).
[9] P. Kirsch, M. B. Assouar, O. Elmazria, V. Mortet, P. Alnot, Appl. Phys. Lett. **88**, 223504 (2006).

[10] D. Neculoiu, A. Müller, G. Deligeorgis, A. Dinescu, A. Stavrinidis, D. Vasilache, A. M. Cismaru, G. E. Stan, G. Konstantinidis, Electron. Lett. **45**, 1196 (2009).

[11] L. Khine, J.B.W. Soon, J.M. Tsai, Solid-State Sensors, Actuators and Microsystems Conference (Transducers), Beijing (China) 16th International, pp. 526–529 (2011).

[12] F. Martin, M. E. Jan, B. Belgacem, Thin Solid Films **514**, 341 (2006).

[13] G. Wingqvist, J. Bjurström, L. Liljeholm, V. Yantchev, I. Katardjiev, Sens. Actuator B-Chem. **123**, 466 (2007).

[14] G. E. Stan, C. O. Morosanu, D. A. Marcov, I. Pasuk, F. Miculescu, G. Reumont, Appl. Surf. Sci. **255**, 9132 (2009).

[15] G. E. Stan, I. Pasuk, A. C. Galca, A. Dinescu, Dig. J. Nanomater. Biostruct. 5, 1041 (2011).

[16] S. Hong, E. Kim, B.-S. Bae, K. No, S.-C. Lim, S.-G. Woo, Y.-B. Koh, J. Vac. Sci. Technol. A **14**, 2721 (1996).

[17] K. Wasa, M. Kitabatake, H. Adachi. Thin film materials technology: Sputtering of compound materials, Noyes Publications (2003).

[18] A. Fardeheb-Mammeri, M. B. Assouar, O. Elmazria, C. Gatel, J-J. Fundenberger, B. Benyoucef, Diam. Relat. Mat. **17**, 1770 (2008).

[19] C.-J. Chung, Y.-C. Chen, C.-C. Cheng, K.-S. Kao, Appl. Phys. A **94**, 307 (2009).

[20] J. Xiong, H.-S. Gu, W. Wu, M.-Z. Hu, P.-F. Du, H. Xie, J. Electron. Mater. **40**, 1578 (2011).

[21] D. Deniz, T. Karabacak, J. M. E. Harper, J. Appl. Phys. **103**, 083553 (2008).

[22] S. Saito, K. Inoue, M. Takahashi, J. Appl. Phys. **109**, 07B753 (2011).